Liquid Crystals
Publication details, including instructions for authors and subscription information:
http://www.informaworld.com/smpp/title~content=t713926090

Computer simulation of elongated bipolar nematic droplets II. External field aligned normal to the droplet axis of symmetry

Philip K. Chan[a]
[a] Department of Chemistry, Biology and Chemical Engineering, Ryerson Polytechnic University, 350 Victoria Street, Toronto, Ontario, Canada M5B 2K3,

Online publication date: 06 August 2010

To cite this Article Chan, Philip K.(2001) 'Computer simulation of elongated bipolar nematic droplets II. External field aligned normal to the droplet axis of symmetry', Liquid Crystals, 28: 2, 207 — 215
To link to this Article: DOI: 10.1080/02678290010004993
URL: http://dx.doi.org/10.1080/02678290010004993

LIQUID CRYSTALS, 2001, VOL. 28, NO. 2, 207–215

Computer simulation of elongated bipolar nematic droplets II. External field aligned normal to the droplet axis of symmetry†

PHILIP K. CHAN

Department of Chemistry, Biology and Chemical Engineering,
Ryerson Polytechnic University, 350 Victoria Street, Toronto, Ontario,
Canada M5B 2K3; e-mail: p4chan@acs.ryerson.ca

(*Received 13 April 2000; accepted 21 June 2000*)

Numerical results from the modelling and computer simulation of the magnetic-induced director reorientation dynamics in elongated bipolar nematic droplets are presented in this paper. The magnetic field is applied normally to the droplet axis-of-symmetry direction, which is one possible scenario found in applications of polymer dispersed liquid crystal (PDLC) films. This case has not yet been studied numerically, and its understanding is far from complete. The model is composed of the Leslie–Ericksen and Frank continuum theories and is solved in two dimensions since bipolar nematic droplets exhibit mirror symmetry in certain planes. The numerical results replicate frequently reported experimental observations on the performance of PDLC films. These observations include the ubiquitous exponential increase followed by saturation in light transmittance as the external applied field increases, and the exponential increase (decrease) followed by saturation as time increases in the on (off)-state. Furthermore, in contrast to current understanding for both the on- and off-states, the model predicts that the directors in the centre (surface) region of the droplet exhibit a dead time (no dead time) before reorientation. The numerical results presented in this paper provide a better understanding of the director reorientation dynamics in elongated bipolar nematic droplets; this can be used to optimize the design and performance of devices using PDLC films.

1. Introduction

Nematic liquid crystals in confined geometries, such as elongated droplets, are of interest to both academic and industrial researchers [1–12] who are interested in the nematic director configuration inside a droplet; the director is defined as the local average molecular orientation [13]. For instance, the effects that the complex coupling of bulk, surface and external forces have on the director configuration within a droplet is mainly an academic problem. Industrial researchers are more interested in determining how they can control the director configuration within a droplet to optimize product performance. Recently, there has been a surge in research on nematic droplets, primarily due to their usage in polymer dispersed liquid crystal (PDLC) films [14–24]. Electronic applications using PDLC films are part of a group of novel systems that form the next generation of liquid crystal display (LCD) technologies.

PDLC films have excellent electro-optical properties, and are used in commercial applications ranging from simple switchable windows to complex billboards and flat panel television screens. The films consist of nematic liquid crystals with positive dielectric anisotropy confined in micron-size bipolar droplets, that are dispersed uniformly in a solid polymer matrix. The director configuration in a bipolar droplet consists of directors anchored tangentially to the surface and two point defects located at each end of the axis of symmetry. PDLC films are formed by the thermally-induced and polymerization-induced phase separation methods, and the emulsification method [3, 4, 14, 15, 18–24]. Depending on the film fabrication conditions, the droplet shape can range from being spherical to elongated, and the bipolar droplet axis of symmetry can be oriented anywhere from along the normal of the film plane to within the film plane.

In their natural (or off-) state, PDLC films are opaque. However, they become transparent in the on-state when an external electric field is applied normally to them. This electro-optic property is due to the director configuration within the bipolar droplets responding to the external electric field. It has been noted that similar optical properties are obtained if a magnetic field is used instead of an electric field [16]. In the off-state, the director configuration is bipolar, which results from the minimization of the bulk elastic free energy. In the on-state, however, the bulk directors reorient and, at

† For part I see reference [11].

Liquid Crystals ISSN 0267-8292 print/ISSN 1366-5855 online © 2001 Taylor & Francis Ltd
http://www.tandf.co.uk/journals
DOI: 10.1080/02678290010004993

sufficiently high external field strengths, are all aligned parallel to the external field direction. Consequently, in order to optimize the performance of electronic products utilizing PDLC films, it is important to understand the dynamics of the evolving director configuration in bipolar droplets in the on- and off-states. This understanding, however, is far from complete.

A survey of the literature indicates that there has been some experimental [3, 5, 7] and numerical [6, 8–12] work on bipolar nematic droplets. This includes the successful dynamical modelling and simulation work of Chan and Rey [10, 11] performed on the director reorientation dynamics in spherical and elongated bipolar nematic droplets, due to a magnetic field aligned parallel to the droplet axis of symmetry direction. We were able to replicate frequently reported experimental observations on the operation of PDLC films, and provide insights on optimization of the usage of these films when the external field is aligned parallel to the droplet axis of symmetry direction. These studies represent one of two extreme cases of droplet axis of symmetry direction, which were mentioned above. The other extreme case where an external field is applied normally to a bipolar nematic droplet (i.e. the axis of symmetry lies within the film plane) has not yet been studied numerically, and, at present, experimental work published in the literature is far from complete in describing the dynamics of the evolving director configuration inside a bipolar droplet in the on- and off-states.

The objective of this paper is to present results from the two-dimensional simulation of a model composed of the Leslie–Ericksen continuum theory for bulk director reorientation dynamics and the Frank continuum theory for the elastic free energy density [13]. The model is a modification of the one we [10, 11] used previously, and is used to simulate the transient director configuration in an elongated bipolar nematic droplet when a magnetic field is applied normally to the droplet axis of symmetry. The elongated droplet is represented in two dimensions as an ellipse with aspect ratio of 1.5.

The rest of this paper is organized as follows. Section 2 presents the model equations used in this paper; results are presented and discussed in § 3; conclusions are given in § 4.

2. Governing equations

The formulation of the model used in this paper follows closely the derivation of the model used previously to study the case where the magnetic field is applied along the droplet axis of symmetry in both spherical and elongated bipolar nematic droplets [11]. A brief description of the Leslie–Ericksen and Frank continuum theories has already been given in [11], in which the derivation considers the cross-section of a spherical (elongated) droplet as a circle (an ellipse). This is shown in figure 1, which also defines the cylindrical coordinate system. The cross-section of the spherical droplet is represented by a circle with radius R and area $A_c = \pi R^2$. The cross-section of the elongated droplet is represented by an ellipse with minor axis length a, major axis length b and area $A_e = \pi ab$. In [11], we limited the investigation to spherical and elongated droplets with equal cross-sectional areas (i.e. $A_c = A_e$). An aspect ratio can be defined for the ellipse as $c = b/a$ and, for academic reasons, is restricted to $c = 1.5$ in this paper. This value is consistent with experimental observations by Drzaic and Muller [4]. They found that for a polyvinylalcohol film containing liquid crystals formed by the emulsification method, the aspect ratio range is $1.1 \leqslant c \leqslant 2.0$, and that $c = 1.7$ for most droplets.

Since there is mirror symmetry about the r-z plane in bipolar droplets, the directors in the r-z plane are affected identically by directors located at mirror locations on either side of this plane. Moreover, the directors in the r-z plane will only be able to rotate within this plane. Consequently, a two-dimensional model can be used to describe and understand the general trends, and compare different cases of the magnetic-induced director reorientation dynamics in bipolar nematic droplets. A

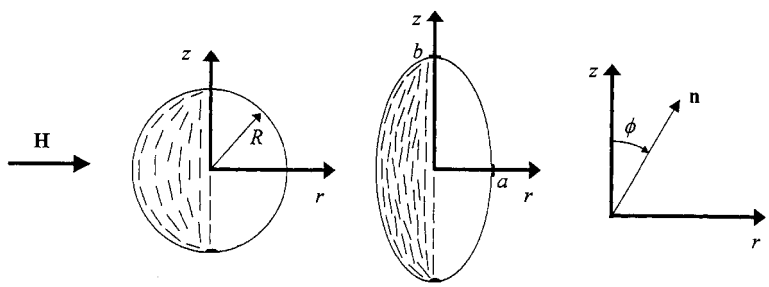

Figure 1. Schematic representation of the cross-section of a spherical droplet (represented by a circle) and an elongated droplet (represented by an ellipse), and definition of the cylindrical coordinate system. The z-axis is along the bipolar droplet axis of symmetry, which is the line joining the two point defects. R is the circle radius, a and b are, respectively, the minor and major axis lengths of the ellipse, ϕ is the orientation angle of the director **n**, and **H** is the magnetic field.

three-dimensional model will only improve the accuracy; it will not change the general trends that are of interest in this paper.

The direction of the magnetic field **H** is normal to the droplet axis of symmetry, and its components are:

$$\mathbf{H} = (H, 0, 0). \tag{1}$$

It is assumed that the director reorientation-induced backflows are negligible since the characteristic times of the velocity changes are much shorter than those of the director [25]. The director field is expressed in terms of the orientation angle ϕ measured from the z-axis as follows:

$$\mathbf{n}(r, z, t) = (\sin \phi(r, z, t), 0, \cos \phi(r, z, t)) \tag{2}$$

where the unit length constraint $\mathbf{n} \cdot \mathbf{n} = 1$ is automatically satisfied.

The equation that governs the behaviour of the orientation angle ϕ is the θ-component of the torque balance; see equation (1) in [11]. By incorporating equations (1) and (2) above with equations (1) to (6) and (9) from [11], the following dimensionless, time-dependent, two-dimensional, non-linear partial differential equation is obtained to describe the magnetic-induced director reorientation dynamics:

$$\frac{\partial \phi}{\partial t^*} = \kappa_1 + \kappa_2 \frac{\partial \phi}{\partial r^*} + \kappa_3 \frac{\partial \phi}{\partial r^*} \frac{\partial \phi}{\partial r^*} + \kappa_4 \frac{\partial^2 \phi}{\partial r^{*2}} + \kappa_5 \frac{\partial \phi}{\partial z^*} + \kappa_6 \frac{\partial \phi}{\partial z^*} \frac{\partial \phi}{\partial z^*} + \kappa_7 \frac{\partial^2 \phi}{\partial z^{*2}} + \kappa_8 \frac{\partial \phi}{\partial r^*} \frac{\partial \phi}{\partial z^*} + \kappa_9 \frac{\partial^2 \phi}{\partial r^* \partial z^*} + \frac{1}{2} Z_0 \sin(2\phi) \tag{3}$$

where the spatially- and angle-dependent elastic functions $\{\kappa_i\}$, where $i = 1, \ldots, 9$, are given in [11]. The dimensionless Zocher number Z_0 gives the relative magnitude of magnetic to elastic torques; it is used in this paper to represent the strength of the external field. The superscript asterisks denote dimensionless variables. The only difference between equation (3) and the governing equation used previously in [11] is in the algebraic sign in front of the term containing the Zocher number, i.e. the last term in equation (3). This difference arises from the fact that these two equations describe extreme cases where the magnetic fields are normal to each other; i.e. the magnetic field is applied normally (parallel) to the droplet axis of symmetry in this paper (in [11]). As shown later in this paper, this simple minor change requires the director configuration within the droplets to evolve differently than that observed in [11].

The initial and boundary conditions used here attempt to mimic reality by including thermal fluctuations in the director orientation. It should be noted that we did not use these fluctuating conditions in [11]. This is done by adding a random number to each orientation angle in the initial and boundary conditions, as follows:

$$\phi = \phi_0(r^*, z^*) \pm \eta\varepsilon \quad \text{at} \quad t^* = 0, \quad -a^* \leqslant r^* \leqslant a^*, \quad -b^* \leqslant z^* \leqslant b^* \tag{4a}$$

$$\phi = -\tan^{-1}\left(\frac{z^*}{r^*}\right) \pm \eta\varepsilon \quad \text{at} \quad t^* > 0, \quad -a^* \leqslant r^* < 0, \quad z^* = (b^{*2} - c^2 r^{*2})^{1/2} \tag{4b}$$

$$\phi = -\tan^{-1}\left(\frac{z^*}{r^*}\right) \pm \eta\varepsilon \quad \text{at} \quad t^* > 0, \quad 0 < r^* \leqslant a^*, \quad z^* = (b^{*2} - c^2 r^{*2})^{1/2} \tag{4c}$$

$$\phi = \frac{\pi}{2} \pm \eta\varepsilon \quad \text{at} \quad t^* > 0, \quad r^* = 0, \quad z^* = \pm b^*. \tag{4d}$$

In equation (4), ε is a random number determined using a standard random number generator and is within the range $0 \leqslant \varepsilon \leqslant 1$; η is a factor that controls the magnitude of the fluctuation. The choice of the algebraic operation $\pm$ is determined randomly by using a random number generator with a different seed than that used to generate ε. If the random number generated is less than 0.5, the sign is negative; otherwise, it is positive. Equation (4d) states that the two poles are represented with directors oriented at $\pi/2$ radians; this can be done since the poles are expected to vanish once the directors begin rotating in the on-state. The dimensionless lengths a^* and b^* are related to the aspect ratio c if the condition $A_c = A_e$ is made [11], which are:

$$a^* = \frac{1}{\sqrt{c}} \tag{5a}$$

$$b^* = \sqrt{c}. \tag{5b}$$

The dimensionless total free energy is obtained by combining equations (1) and (2) above with equations (5), (6) and (9) from [11]. It is expressed as follows:

$$F^* = F_d^* + F_m^* + F_s^* \tag{6}$$

where

$$F_m^* = -\pi Z_0 \iint r^* \sin^2 \phi \, dr^* \, dz^*. \tag{7}$$

The expression for F_d^* is given in [11]; the expression for F_m^* is different from that given in [11] because of the different orientations of the magnetic field. Note that an expression for F_s^* is not given since there is no surface

contribution to the total free energy when the director is anchored along the easy axis direction, which is the case for the bipolar droplets studied in this paper.

The parameter values that are used in this paper are: $K^*_{11} = 0.6667$, $K^*_{33} = 1.3333$, $c = 1.5$, $0 \leqslant Z_0 \leqslant 2500$ and $\eta = 0.1$. They are used in equations (3) to (7) to determine the transient director configuration $\phi = \phi(r^*, z^*, t^*)$ and dimensionless total free energy F^*. The values for the elastic constants were specifically chosen to satisfy the condition $(K_{33}/K_{11}) > 1$ which is required for a bipolar droplet to form [19]. Equations (3) to (5) are solved using the method of solution described in [11].

3. Results and discussion

Numerical results from the computer simulations indicated above are presented and discussed in this section, which is divided into three parts. The first part defines a mean magnitude of the orientation angle that can be computed using the numerical results obtained from the simulation of the model derived above. The mean angle can be used to compare numerical results with experimental light transmittance results found in the literature for PDLC films. The last two parts contain results for the on-state and off-state simulations.

3.1. *Mean orientation angle*

A mean magnitude of the orientation angle can be defined to facilitate discussion of numerical results and comparison with published experimental results; this is expressed as follows:

$$\langle \| \phi \| \rangle = \frac{1}{\pi} \int_{-b^*}^{b^*} \int_{-a^*}^{a^*} |\phi| \, \mathrm{d}r^* \, \mathrm{d}z^*. \tag{8}$$

In the limit where all the bulk and surface directors are aligned along the z-axis, $\langle \| \phi \| \rangle = 0$. On the other hand, $\langle \| \phi \| \rangle = \pi/2$ radians if all the bulk and surface directors are aligned along the r-axis. $\langle \| \phi \| \rangle$ can be used to relate numerical simulation results to experimental light transmittance results found in the literature for PDLC films [10, 11, 14], since it has already been noted that the optical phenomena of PDLC films can be explained by looking at individual droplets [3]. In the off-state, both light transmittance and $\langle \| \phi \| \rangle$ have low values. On the other hand, both light transmittance and $\langle \| \phi \| \rangle$ have high values in the on-state. This means that the light transmittance of a PDLC film increases with $\langle \| \phi \| \rangle$ for the case where the external field is applied normally to the droplet axis of symmetry direction. This is in contrast to the case where the magnetic field is applied parallel to the droplet axis of symmetry direction [11]. Lastly, $\langle \| \phi_{ss} \| \rangle$ denotes the mean magnitude of the orientation angle at steady state in the on- and off-states.

3.2. *On-state*

Figure 2 shows the director configuration of the bipolar nematic droplet used in the computer simulations presented in this paper. This configuration satisfies all the conditions given in equation (4) and is used as the initial condition for the on-state. It is also the steady state director configuration in the off-state.

Figure 3 is a plot of $\langle \| \phi \| \rangle$ versus dimensionless time t^* during the on- and off-states for the following Zocher numbers: $Z_0 = 10$ (solid line), $Z_0 = 500$ (dotted line) and $Z_0 = 2500$ (dashed line). This figure shows that the transient director reorientation phenomena in the on-state can be divided into three regimes depending on the magnitude of Z_0. Two plateaus form in the $\langle \| \phi \| \rangle$–$t^*$ curve at low Zocher numbers ($Z_0 = 10$); however, only one plateau forms at high Zocher numbers ($Z_0 = 2500$). Moreover, the $\langle \| \phi \| \rangle$–$t^*$ curve shows intermediate features at intermediate Zocher numbers ($Z_0 = 500$). The presence

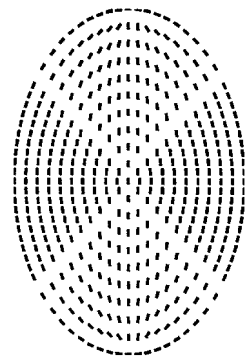

Figure 2. Director configuration of the bipolar nematic droplet used in this paper. This configuration is the initial condition for the on-state and the steady state configuration in the off-state. The poles have been replaced with directors.

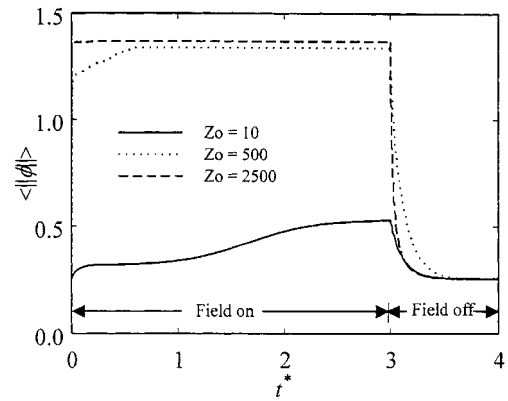

Figure 3. Mean magnitude of the orientation angle $\langle \| \phi \| \rangle$ versus dimensionless time t^* for low, intermediate and high values of the Zocher number Z_0. The magnetic field is on during the time range $0 \leqslant t^* \leqslant 3$, but is off during the time range $3 < t^* \leqslant 4$. The same curves are obtained when the magnetic field is turned on and off repeatedly, as required in PDLC film operation.

of these three regimes can be explained by examining the time evolution of ϕ at two strategically placed locations in the ellipse. The directors at these two locations give a sense of director reorientation dynamics within the ellipse.

Figure 4 shows the time evolution of ϕ at point 1 (solid line) with coordinates (0, 0) and point 2 (dashed line) with coordinates (0.48, 0.67) for the corresponding on- and off-states shown in figure 3. In addition, figure 4 contains graphs for: (*a*) $Z_0 = 10$, (*b*) $Z_0 = 500$, and (*c*) $Z_0 = 2500$. The time evolution of ϕ for $Z_0 = 10$ shows that at very early times ($t^* < 0.2$) the director at point 2 reorients at a very fast rate, while the director at point 1 initially exhibits a dead time followed by sluggish reorientation. At $t^* = 0.2$, the rate of reorientation of the director at point 2 decreases and reorientation continues at about the same slow rate as the director at point 1; this leads to the formation of the first plateau at $t^* = 0.2$ in figure 3. The rate of director reorientation at point 1 increases at $t^* = 1.0$; the directors at both points cease to reorient at $t^* = 3.0$. This leads to the formation of the second plateau in figure 3. Figure 4 (*b*) ($Z_0 = 500$) shows that the director at point 2 reorients first and does this at a very fast rate. The director at point 1 has a dead time, after which it also reorients at a very fast rate. Because of its dead time, the director at point 1 reaches only about half-way to its steady state orientation when the director at point 2 has reached its steady state. This explains why the $\langle \| \phi \| \rangle - t^*$ curve for $Z_0 = 500$ in figure 3 exhibits a change in slope at $t^* = 0.05$. Lastly, the rate of reorientation is the same and very fast for the directors at points 1 and 2 for high Zocher numbers, as shown in figure 4 (*c*) for $Z_0 = 2500$. Although it is difficult to see in this figure, the director at point 1 exhibits a dead time initially, as for $Z_0 = 10$ and 500. Because this dead time is small and the orientation angle at both locations follows almost identically the same time evolution pattern, no plateau can form in the $\langle \| \phi \| \rangle - t^*$ curve shown in figure 3.

The above discussion states that the director at point 1 exhibits a dead time in the on-state while none is observed for point 2. This can be explained by examining the governing equation, which is the balance of elastic, viscous and magnetic torques; see equation (3). The last

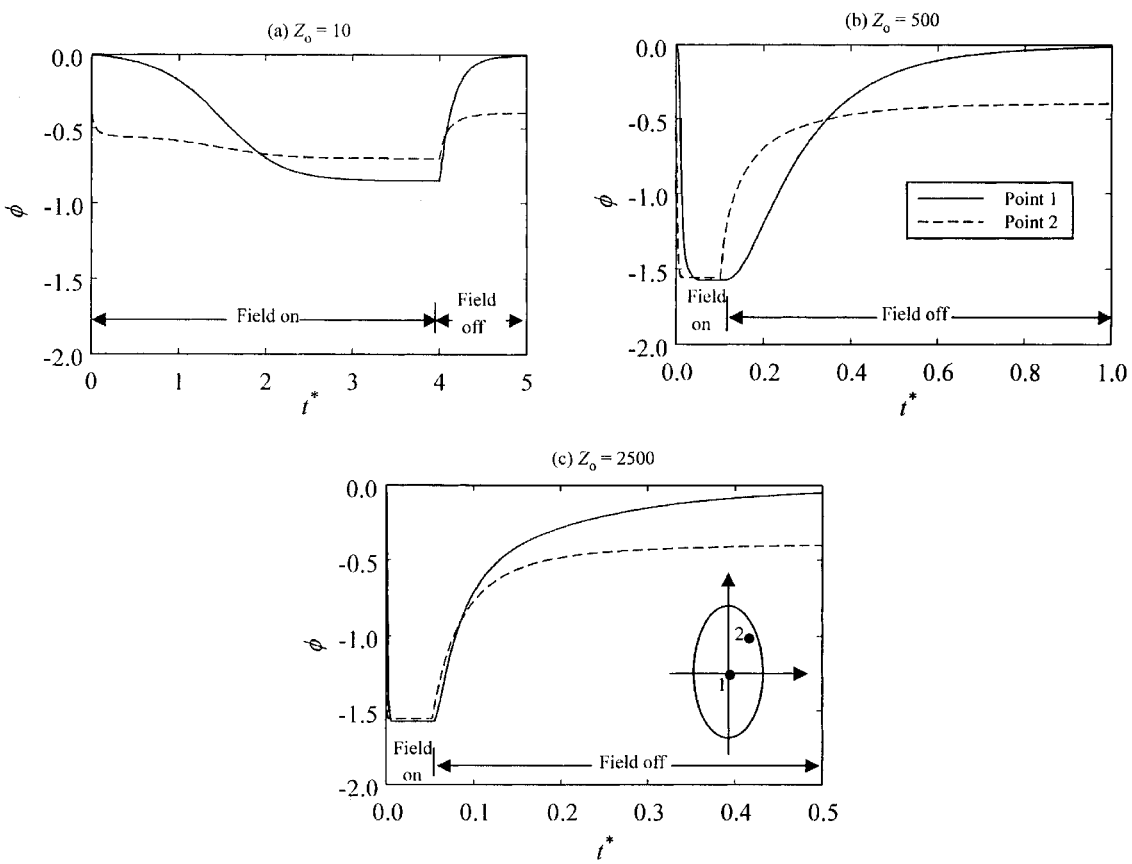

Figure 4. Orientation angle ϕ versus dimensionless time t^* in the on- and off-states for the following Zocher numbers: (*a*) $Z_0 = 10$, (*b*) $Z_0 = 500$, and (*c*) $Z_0 = 2500$. The time evolution of ϕ is given for the following two locations: point 1 (solid line) with coordinates (0, 0) representing the centre region, and point 2 (dashed line) with coordinates (0.48, 0.67) representing the surface regions.

term in equation (3), which contains Z_0, is the magnetic torque contribution. Since the director at point 1 is initially normal to the external field direction with $\phi = 0$, there is no magnetic torque acting on the director to cause it to reorient. Conversely, there is a magnetic torque acting on the director at point 2 since the director is not initially normal to the external field direction ($\phi \neq 0$). It is the magnetic-induced director reorientation at locations where $\phi \neq 0$ that induces, through elastic and viscous torques, the reorientation of directors at locations where $\phi = 0$. Therefore, the director at point 2 (and at any other locations where $\phi \neq 0$) will always reorient before the director at point 1 (and at any other locations where $\phi = 0$), and this difference in time is the dead time. This observation of a dead time for directors that are aligned normally to the external field direction has also been observed by Shabanov *et al.* [12] in their numerical simulation of bipolar droplets with fixed poles. However, this observation is different from the qualitative model proposed by Drzaic [3], which states that the directors in the centre region of a bipolar droplet reorients first followed later by the directors in the surface region, on application of an external field that is normal to the PDLC film. A plausible reason for this difference is the shape of the droplets being investigated. This paper studies model elongated droplets where the cross-section is an ellipse and the droplet axis of symmetry lies within the film plane. Conversely, Drzaic [3] worked with droplets that are not perfectly elongated and have surface irregularities. Because of this, the droplet axis of symmetry may also not lie within the film plane.

The corresponding steady state director configurations at $Z_0 = 10$, 500 and 2500 are shown in figure 5. The initial director configuration for all three Z_0 values is shown in figure 2. Comparison of these director configurations indicates that at low Zocher numbers ($Z_0 = 10$) the directors in the centre region reorient to some extent toward the magnetic field direction, while the directors in the surface region do not. This difference between the centre and surface regions, however, decreases upon increasing Z_0. At intermediate Zocher numbers ($Z_0 = 500$), the directors in the centre region are aligned along the magnetic field direction. Moreover, the directors in the surface region have also reoriented significantly toward the magnetic field direction. At high Zocher numbers ($Z_0 = 2500$), all the directors within the droplet are generally aligned along the magnetic field direction. This phenomenon is due to the competition between droplet surface and external field effects and can be explained using the magnetic coherence length ξ [13]. This length represents the effect that the surface has on the directors and is equal to the thickness of the transition layer where the director varies from the surface director orientation to the bulk director orientation. In addition, ξ is inversely proportional to the external field strength ($\xi \propto Z_0^{-1}$) and was originally defined for an infinite liquid crystal sample on a flat surface. It can, however, be adapted for a droplet [19]. In the limit where $Z_0 = 0$ ($Z_0 \to \infty$), $\xi \to \infty$ ($\xi = 0$) and surface (external field) effects dominate. The directors in the surface region do not reorient for $Z_0 = 10$ because ξ is relatively large (i.e. surface effects dominate). Upon increasing Z_0 to 500, ξ decreases and the directors reorient significantly in the surface region. At $Z_0 = 500$, both surface and external field effects dominate. Lastly, $\xi \to 0$ (i.e. no surface effects) at $Z_0 = 2500$ and the

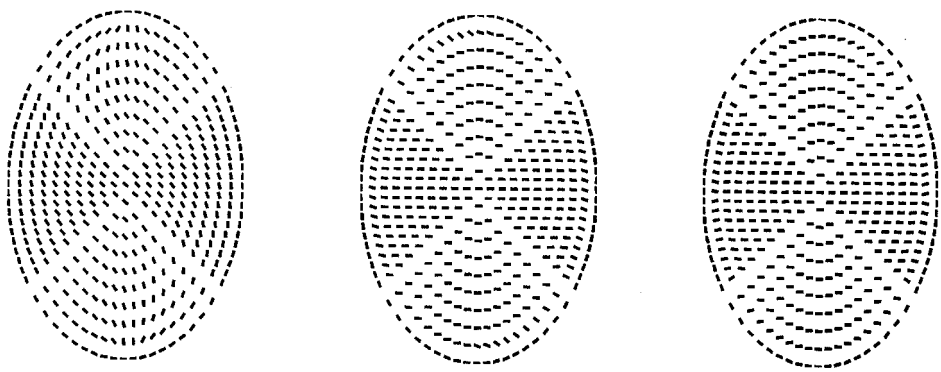

Figure 5. Steady state director configurations in the on-state for the following Zocher numbers: (*a*) $Z_0 = 10$, (*b*) $Z_0 = 500$, and (*c*) $Z_0 = 2500$. The director configuration at low Zocher numbers ($Z_0 = 10$) reorients slightly, while the director configuration inside the droplet is almost uniform at high Zocher numbers ($Z_0 = 500$ and 2500). These results are consistent with experimental observations reported in the literature. These configurations also represent the initial state of the off-state dynamics discussed in this paper.

directors in the surface region are generally aligned with the directors in the centre region along the external field direction.

Frequently reported experimental results for PDLC film light transmittance are usually given for very high external field strengths to ensure maximum light transmittance in the on-state. One of these experimental observations shows that the light transmittance increases exponentially and then saturates with time in the on-state [18]. Figure 3 can be used to explain this observation by recalling that light transmittance increases with $\langle \| \phi \| \rangle$. Moreover, the curve for $Z_0 = 2500$ can be used since this Zocher number value is sufficient to create maximum bulk director reorientation ($\phi = \pi/2$ rad) as shown in figure 5. Consequently, the exponential rise and saturation of light transmittance with time is due to the exponential increase and saturation in $\langle \| \phi \| \rangle$ with time.

Figure 6 is a plot of $\langle \| \phi_{ss} \| \rangle$ versus Z_0; it shows that $\langle \| \phi_{ss} \| \rangle$ increases exponentially with Z_0 at low Zocher numbers but then saturates at high Zocher numbers. This figure can be used to explain the experimental observation that light transmittance from PDLC films increases, then saturates, as the external field strength increases [18]. Consequently, the exponential increase in light transmittance at low external field strengths is due to the exponential increase of $\langle \| \phi_{ss} \| \rangle$ with Z_0 at low Zocher numbers. Moreover, the saturation in light transmittance at high external field strengths is due to the saturation of $\langle \| \phi_{ss} \| \rangle$ with Z_0 at high Zocher numbers.

Before ending the discussion for the on-state, it would be interesting to compare the results presented above with those published in [11] where the magnetic field is aligned parallel to the droplet axis of symmetry direction. As expected, the bulk directors in both cases reorient along their respective magnetic field directions in the on-state for sufficiently high field strengths. This is shown in figure 5 (*c*) above and figure 3 in [11]. These two figures show that the steady-state bulk director configuration is almost uniform and oriented normal to each other; this is because the magnetic fields for these two cases are normal to each other. The bulk directors reorient to $\pi/2$ rad (0 rad) when the magnetic field is aligned normal (parallel) to the droplet axis of symmetry direction. This difference is also reflected in plots of $\langle \| \phi \| \rangle$ versus t^* and $\langle \| \phi_{ss} \| \rangle$ versus Z_0, as shown in figures 3 and 6 above and figures 2 and 6 in [11]. Nevertheless, the numerical results for these two magnetic field cases replicate the following frequently reported experimental observations: (a) the light transmittance increases exponentially at first and then saturates as the externally applied field increases, (b) the light transmittance increases exponentially and then saturates with time in the on-state. This implies that both magnetic field cases can be used in PDLC film applications.

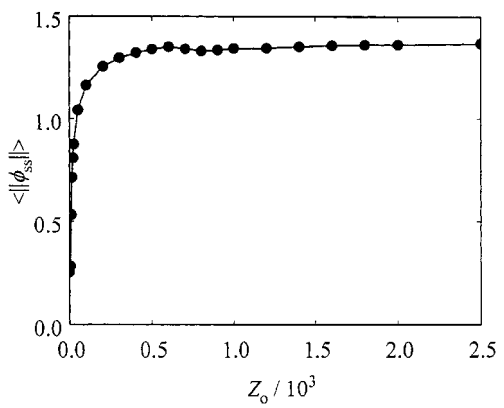

Figure 6. Mean magnitude of the orientational angle at steady state $\langle \| \phi_{ss} \| \rangle$ versus Zocher number Z_0. The exponential rise and saturation exhibited by $\langle \| \phi_{ss} \| \rangle$ as Z_0 increases can be used to explain the frequently reported experimental observation that light transmittance from PDLC films increases exponentially followed by saturation as the external field strength increases, by noting that light transmittance is proportional to $\langle \| \phi_{ss} \| \rangle$.

3.3. *Off-state*

The time evolution of $\langle \| \phi \| \rangle$ in the off-state is given in figure 3 for the following Zocher numbers: $Z_0 = 10$ (solid line), $Z_0 = 500$ (dotted line) and $Z_0 = 2500$ (dashed line). This figure shows that the time evolution of $\langle \| \phi \| \rangle$ decreases exponentially at early times, and then saturates to a steady state value at late times. This observation can be used to explain the frequently reported experimental observation that light transmittance in PDLC films in the off-state decreases exponentially at first before reaching its steady state value asymptotically [18] by recalling that light transmittance is proportional to $\langle \| \phi \| \rangle$. It is also noticed in figure 3 that the rate of change of $\langle \| \phi \| \rangle$ increases with Z_0 at intermediate and high Zocher numbers ($Z_0 = 500$ and 2500). This can be explained by referring to figure 5, which shows the corresponding initial director configuration for the off-state for the three cases show in figure 3. As discussed above, figure 5 also represents the steady state director configuration for the on-state for $Z_0 = 10$, 500 and 2500. Figure 5 shows that the level of distortion in the director configuration increases with Z_0, which is reflected in the dimensionless total stored elastic distortion free energy F_d^* shown in figure 7. The driving force for director reorientation in the off-state is, therefore, the stored elastic distortion free energy; this fact has already been observed experimentally by Drzaic and Muller [4]. The observation that the rate of change of $\langle \| \phi \| \rangle$ increases as Z_0 increases from 500 to 2500 is due to the director

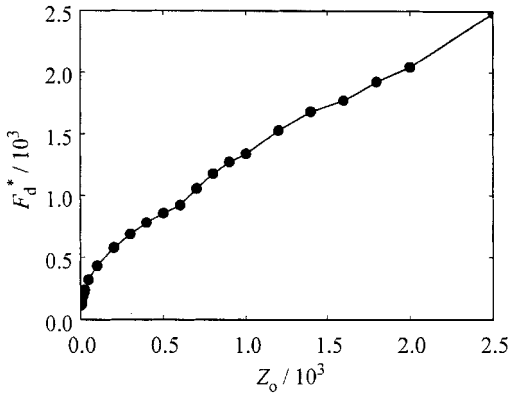

Figure 7. Dimensionless total stored distortion free energy F_d^* versus Zocher number Z_0. The stored distortion free energy is the driving force for director reorientation in the off-state.

configuration becoming more distorted upon increasing Z_0, as shown in figure 5. This increase in distortion increases F_d^* which, as stated by Drzaic and Muller [4], will increase the rate of director reorientation in the off-state.

The time evolution of the orientation angle ϕ in the off-state at coordinates $(0, 0)$ and $(0.48, 0.67)$ is shown in figure 4 for: (*a*) $Z_0 = 10$, (*b*) $Z_0 = 500$ and (*c*) $Z_0 = 2500$. These figures indicate that the directors at both points starts to reorient at the same time in the off-state for low Zocher numbers ($Z_0 = 10$). They also indicate that for intermediate and high Zocher numbers ($Z_0 = 500$ and 2500) there is a dead time for the director at point 1 before it starts to reorient. This can be explained by using figure 5 once more. The director configuration inside a droplet with low Zocher numbers ($Z_0 = 10$) is non-uniform; therefore, in the off-state all directors begin reorienting at the same time. On the other hand, the director configuration inside a droplet at intermediate and high Zocher numbers is almost uniform at the start of the off-state. Since the director at point 1 is in a region of uniformity, it requires torques to be transmitted to it for reorientation. The source of these torques is the reorientation of the directors in the surface region (such as point 2) induced by the relaxation of the stored elastic free energy due to the tremendous distortion in the director configuration near the surface, as shown in figure 5 for $Z_0 = 500$ and 2500. The time taken for the torques to be transmitted to point 1 is the dead time. This observation is different from the qualitative model proposed by Drzaic [3], which states that the directors in the center region of a bipolar droplet reorient first, followed later by the directors in the surface region, on removal of an external field that is normal to the PDLC film. The same reasoning given above for the on-state is offered here for the off-state, which is the difference in shape of the droplets investigated. This paper studies model elongated droplets where the cross-section is an ellipse and the droplet axis of symmetry lies within the film plane. In contrast, Drzaic [3] worked with droplets that were not perfectly elongated and had surface irregularities. Because of this, the droplet axis of symmetry may not lie within the film plane.

Lastly, it would be interesting to compare the results presented above for the off-state with those published previously where the magnetic field is aligned parallel to the droplet axis of symmetry [11]. As with the on-state case, opposite dynamical features are observed in the off-state for these two magnetic field cases. Consider the case where the bulk directors are almost uniformly oriented along the magnetic field direction, which is expected for sufficiently high external field strengths. The bulk directors reorient from an almost uniform configuration of $\pi/2$ rad (0 rad) to some steady-state configuration in the off-state when the magnetic field is normal (parallel) to the droplet axis of symmetry direction. This is reflected in a plot of $\langle \| \phi \| \rangle$ versus t^* as shown in figure 3 above and figure 2 in [11]. Despite this difference, the numerical results for these two cases replicate the experimental observation that the light transmittance decreases exponentially and then saturates with time in the off-state. As already mentioned above for the on-state, this implies that both magnetic field cases can be used in PDLC film applications.

4. Conclusions

This paper has studied the magnetic-induced director reorientation dynamics in elongated bipolar nematic droplets by modelling and computer simulation. Because of mirror symmetry about the *r*-*z* plane, the study was limited to two dimensions. The droplets were represented by ellipses with aspect ratio $c = 1.5$ centred at the origin and in the plane of symmetry.

The numerical results were able to replicate frequently reported experimental observations on the operation of PDLC films. These experimental observations are: (a) the light transmittance increases exponentially at first and then saturates as the externally applied field increases, (b) the light transmittance increases exponentially and then saturates with time in the on-state, and (c) the light transmittance decreases exponentially and then saturates with time in the off-state.

The numerical results for the on-state also indicated that directors which are oriented normally to the external field direction (i.e. $\mathbf{n} \cdot \mathbf{H} = 0$) exhibit a dead time before reorientation starts. These directors are generally in the centre region of the droplet and require viscous and elastic torques to be transmitted from directors undergoing reorientation in the surface region of the droplet where generally $\mathbf{n} \cdot \mathbf{H} \neq 0$. Moreover, the numerical results

for the off-state also indicated that the directors in the surface region generally start reorienting back to their bipolar configuration before the directors in the centre region, due to the enormous curvature at the droplet surface.

The numerical results presented in this paper provide a better understanding of the director reorientation dynamics in bipolar nematic droplets when a magnetic field is applied normally to it, and when the field is turned off after the directors have reached maximum reorientation. This understanding facilitates optimal design and control of PDLC films and electronic products utilizing PDLC technology.

This work is supported by grants from Ryerson Polytechnic University and the Natural Sciences and Engineering Research Council of Canada.

References

[1] Dubois-Violette, E., and Parodi, O., 1969, *J. Phys. (Paris) Colloq.*, **30,** C4-57.
[2] Candau, S., Le Roy, P., and Debeauvais, F., 1973, *Mol. Cryst. liq. Cryst.*, **23,** 283.
[3] Drzaic, P. S., 1988, *Liq. Cryst.*, **3,** 1543.
[4] Drzaic, P. S., and Muller, A., 1989, *Liq. Cryst.*, **5,** 1467.
[5] Wu, B.-G., Erdmann, J. H., and Doane, J. W., 1989, *Liq. Cryst.*, **5,** 1453.
[6] Vilfan, I., Vilfan, M., and Zumer, S., 1989, *Phys. Rev. A*, **40,** 4724.
[7] Jain, S. C., and Rout, D. K., 1991, *J. appl. Phys.*, **70,** 6988.
[8] Huang, W., and Tuthill, G. F., 1994, *Phys. Rev. E*, **49,** 570.
[9] Ding, J., Zhang, H., Lu, J., and Yang, Y., 1995, *Jpn. J. appl. Phys.*, **34,** 1928.
[10] Chan, P. K., and Rey, A. D., 1997, *Liq. Cryst.*, **23,** 677.
[11] Chan, P. K., 1999, *Liq. Cryst.*, **26,** 1777.
[12] Shabanov, A. V., Presnyakov, V. V., Ya Zyryanov, V., and Ya Vetrov, S., 1998, *JETP Lett.*, **67,** 733.
[13] De Gennes, P. G., and Prost, J., 1993, *The Physics of Liquid Crystals*, 2nd Edn (Clarendon Press).
[14] Wu, B.-G., West, J. L., and Doane, J. W., 1987, *J. appl. Phys.*, **62,** 3925.
[15] Doane, J. W., 1990, *Liquid Crystals: Applications and Uses*, Vol. 1, edited by B. Bahadur (World Scientific), pp. 361–395.
[16] Li, Z., Kelly, J. R., Palffy-Muhoray, P., and Rosenblatt, C., 1992, *Appl. Phys. Lett.*, **60,** 3132.
[17] Erdmann, J. H., Lackner, A. M., Sherman, E., and Margerum, J. D., 1993, *J. SID*, **1,** 57.
[18] Montgomery, G. P., Smith, G. W., and Vaz, N. A., 1994, *Liquid Crystalline and Mesomorphic Polymers*, edited by V. P. Shibaev and L. Lam (Springer-Verlag), pp. 149–192.
[19] Drzaic, P. S., 1995, *Liquid Crystal Dispersions* (World Scientific).
[20] Chan, P. K., and Rey, A. D., 1995, *Comput. Mater. Sci.*, **3,** 377.
[21] Chan, P. K., and Rey, A. D., 1995, *Macromol. Theory Simul.*, **4,** 873.
[22] Chan, P. K., and Rey, A. D., 1996, *Macromolecules*, **29,** 8934.
[23] Chan, P. K., and Rey, A. D., 1997, *Macromolecules*, **30,** 2135.
[24] Chan, P. K., 1998, *Recent Res. Devel. macromol. Res.*, **3,** 439.
[25] Blinov, L. M., and Chigrinov, V. G., 1994, *Electrooptic Effects in Liquid Crystalline Materials* (Springer), Chap. 4.